Results from PRad Experiment

Xinzhan Bai
University of Virginia

PRad Collaboration Meeting
12/06/2019

Outline

- Proton charge radius puzzle
- PRad experiment
- Analysis and results
- Summary

Proton Charge Radius Puzzle

- E-p elastic scattering
- Spectroscopy

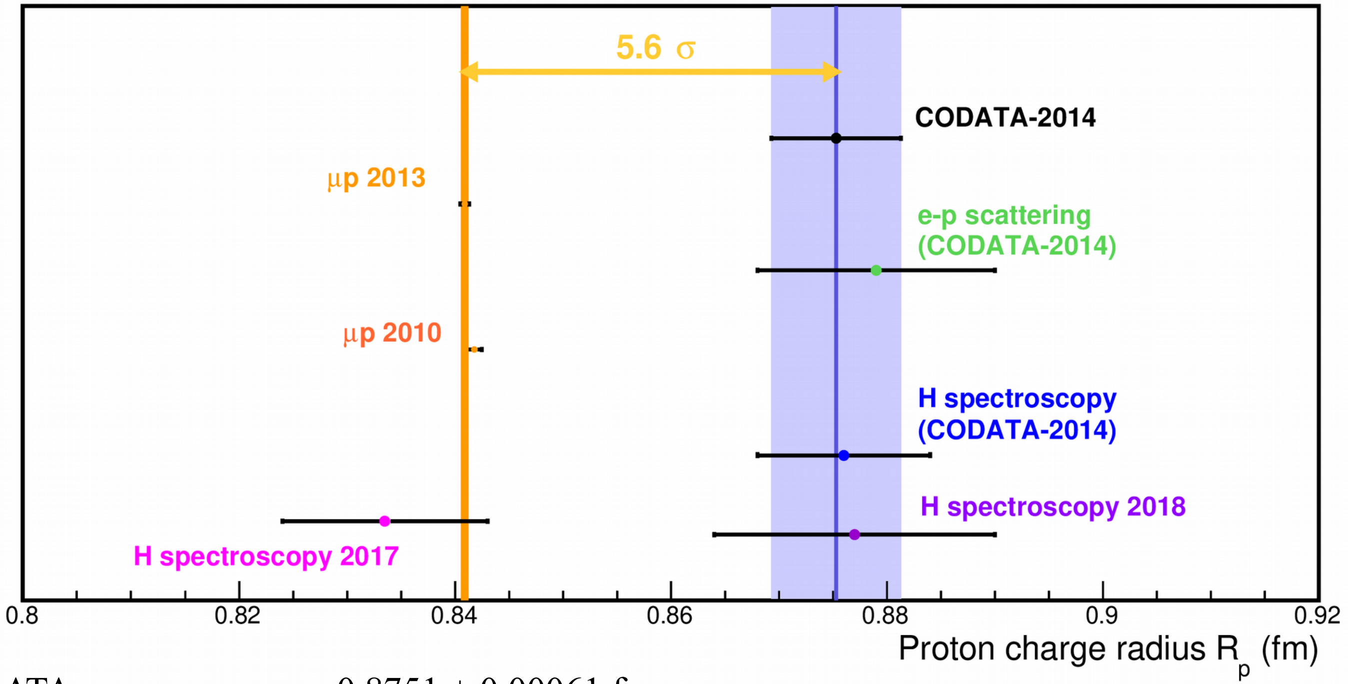

- Combined CODATA average: 0.8751 ± 0.00061 fm
- *ep* scattering average (CODATA): 0.879 ± 0.011 fm
- Muon spectroscopy: 0.8409 ± 0.0004 fm (CREMA 2010, 2013)
- H spectroscopy (2017): 0.8335 ± 0.0095 fm (A. Beyer et al. Science 358 6359 (2017))
- H spectroscopy (2018): 0.877 ± 0.013 fm (H. Fleurbaey et al. PRL 120 183001 (2018))

ep Elastic Scattering

- Elastic ep scattering, in the limit of Born approximation (one photon exchange):

$$\frac{d\sigma}{d\Omega} = \left(\frac{d\sigma}{d\Omega}\right)_{Mott} \left(\frac{E'}{E}\right) \frac{1}{1+\tau} \left(G_E^{p\,2}(Q^2) + \frac{\tau}{\epsilon} G_M^{p\,2}(Q^2)\right)$$

$$Q^2 = 4EE'\sin^2\frac{\theta}{2} \quad \tau = \frac{Q^2}{4M_p^2} \quad \epsilon = \left[1 + 2(1+\tau)\tan^2\frac{\theta}{2}\right]^{-1}$$

- Structure-less proton:

$$\left(\frac{d\sigma}{d\Omega}\right)_{Mott} = \frac{\alpha^2[1 - \beta^2\sin^2\frac{\theta}{2}]}{4k^2\sin^4\frac{\theta}{2}}$$

- G_E and G_M can be extracted using Rosenbluth separation
- For PRad, cross section dominated by G_E

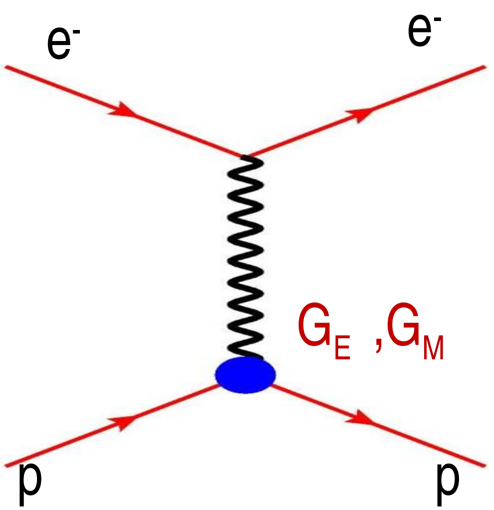

Taylor expansion of G_E at low Q^2

$$G_E^p(Q^2) = 1 - \frac{Q^2}{6}\langle r^2\rangle + \frac{Q^4}{120}\langle r^4\rangle + \ldots$$

Derivative at low Q^2 limit

$$\langle r^2\rangle = -6 \left.\frac{dG_E^p(Q^2)}{dQ^2}\right|_{Q^2=0}$$

PRad Experiment Overview

- PRad goal: measure proton charge radius using ep elastic scattering
- Covers two orders of magnitude in low Q^2 with the same detector setting
    1. ~ 2×10^{-4} – 6×10^{-2} GeV^2
- Unprecedented low Q^2 (~ 2×10^{-4} GeV^2)
    1. Fill in very low Q^2 region
- Normalize to the simultaneously measured Møller scattering process
    1. Best known control of systematics
- Extract the radius with precision from sub-percent cross section measurement

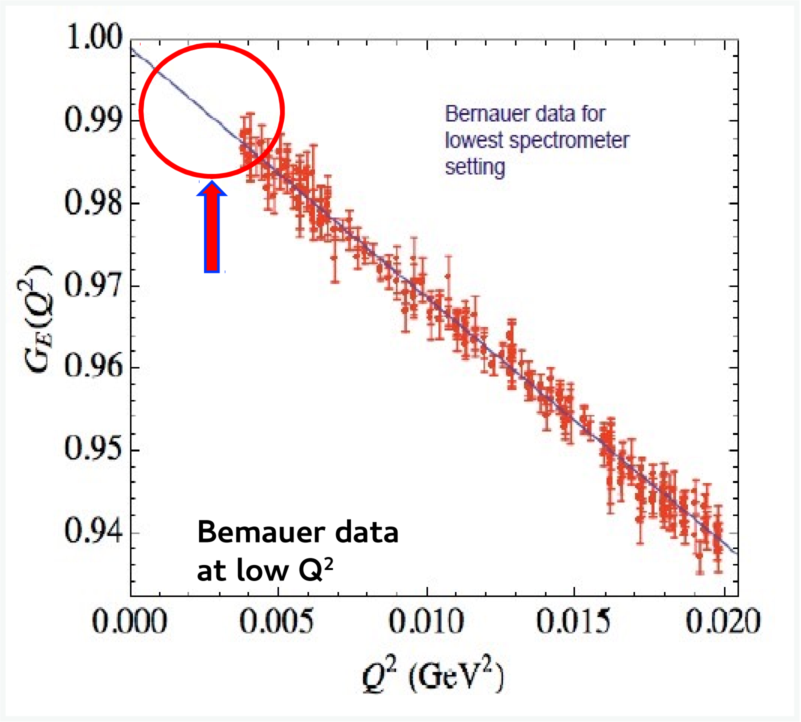

Jefferson Laboratory

PRad experimental data taking May/June 2016
Two beam energies 1.1 GeV and 2.2 GeV

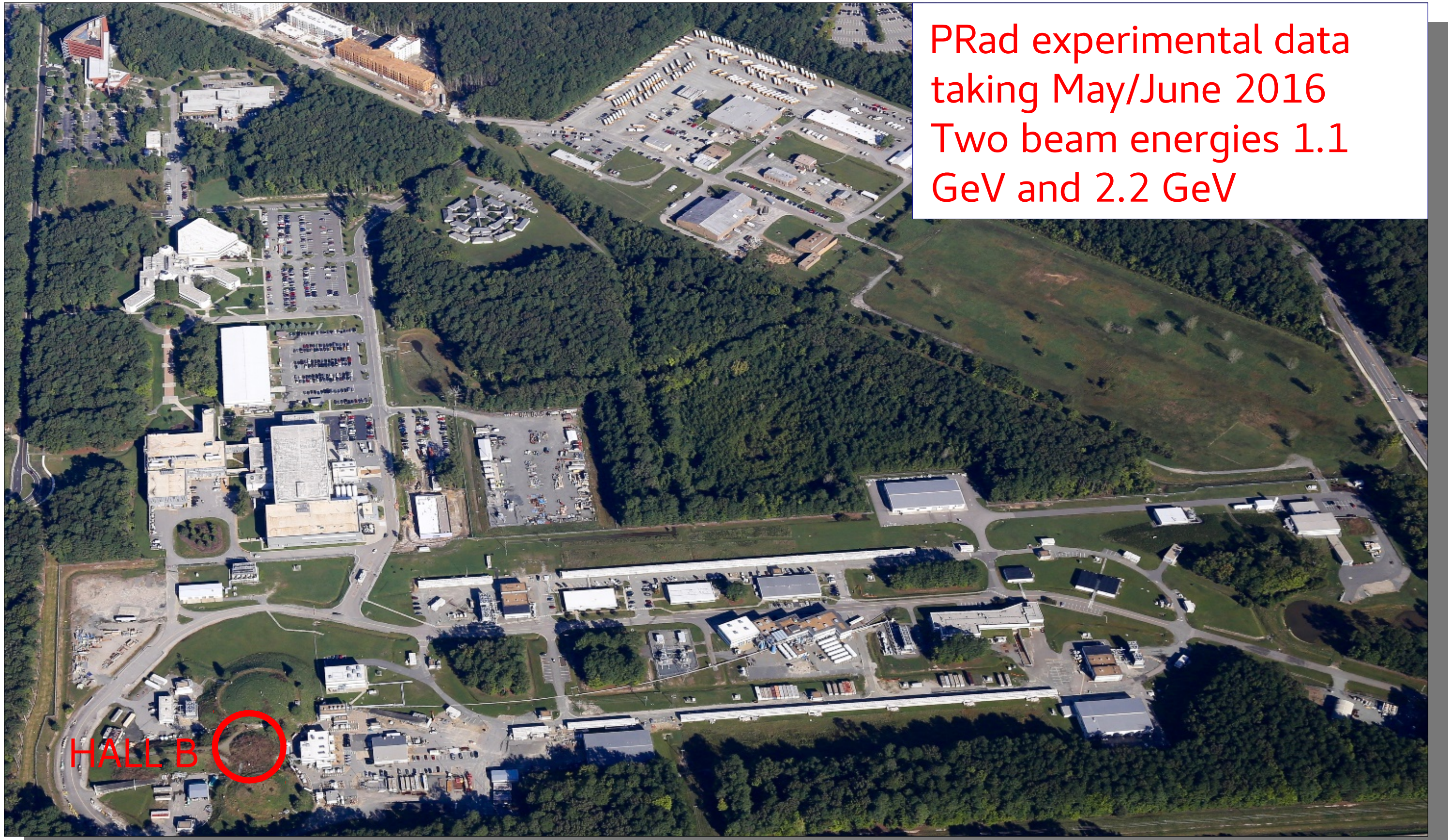

PRad was one of the first experiments to run at Jefferson lab after its major upgrade

PRad Experimental Apparatus

Hall B

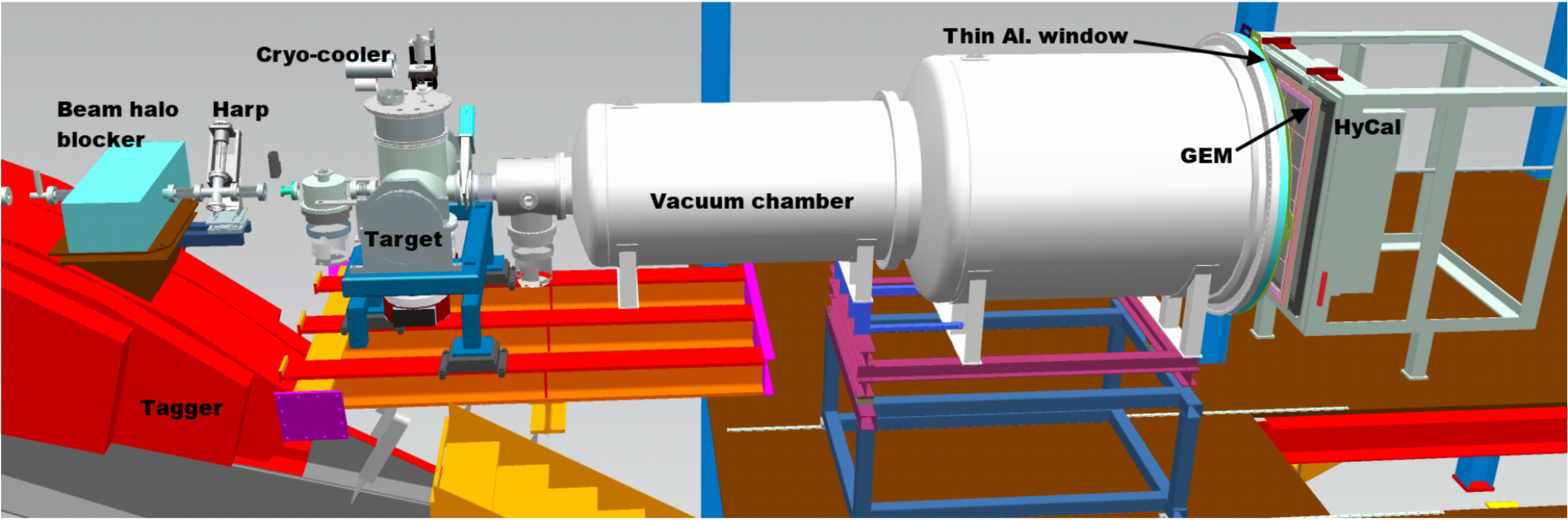

- Windowless H_2 gas flow target
- Vacuum chamber (reduce beam line background)
- Two high resolution (72um), large area (120cm X 120 cm), GEM detectors
- High resolution, large acceptance, hybrid calorimeter ($PbWO_4$ and Pb-Glass)

Spokesperson:
A. Gasparian, H. Gao, D. Dutta, M. Khandaker

Simultaneous detection of ee → ee Moller scattering

- Simultaneous detection of Moller (ee→ee) and (ep→ep) events within the same acceptance

  1) Best control of systematics
  2) Eliminates needs to monitor luminosity
  3) Large Q^2 range in a single setting
  4) Fill in the very low Q^2 range

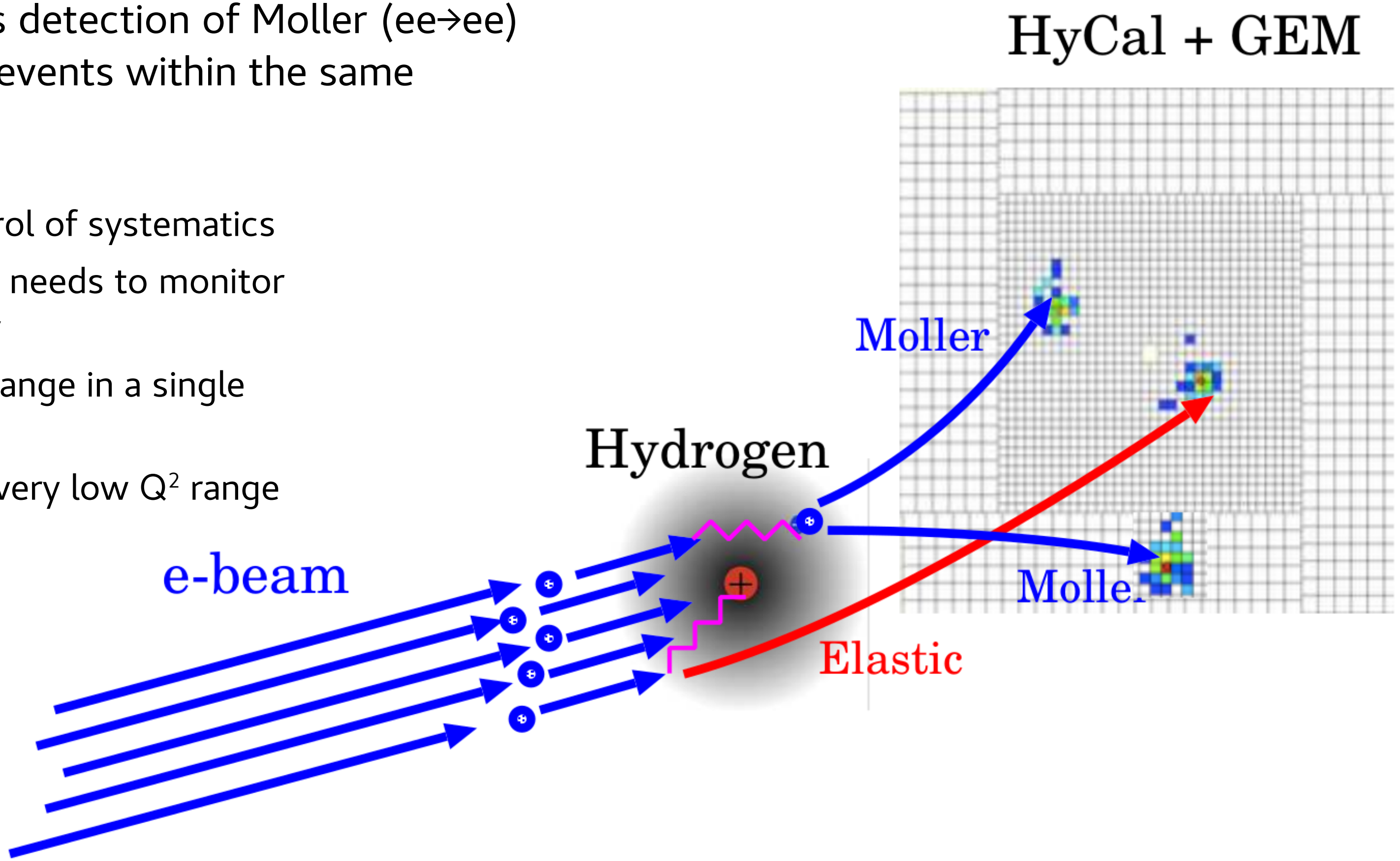

PRad Experimental Apparatus

PRad Setup (Side View)

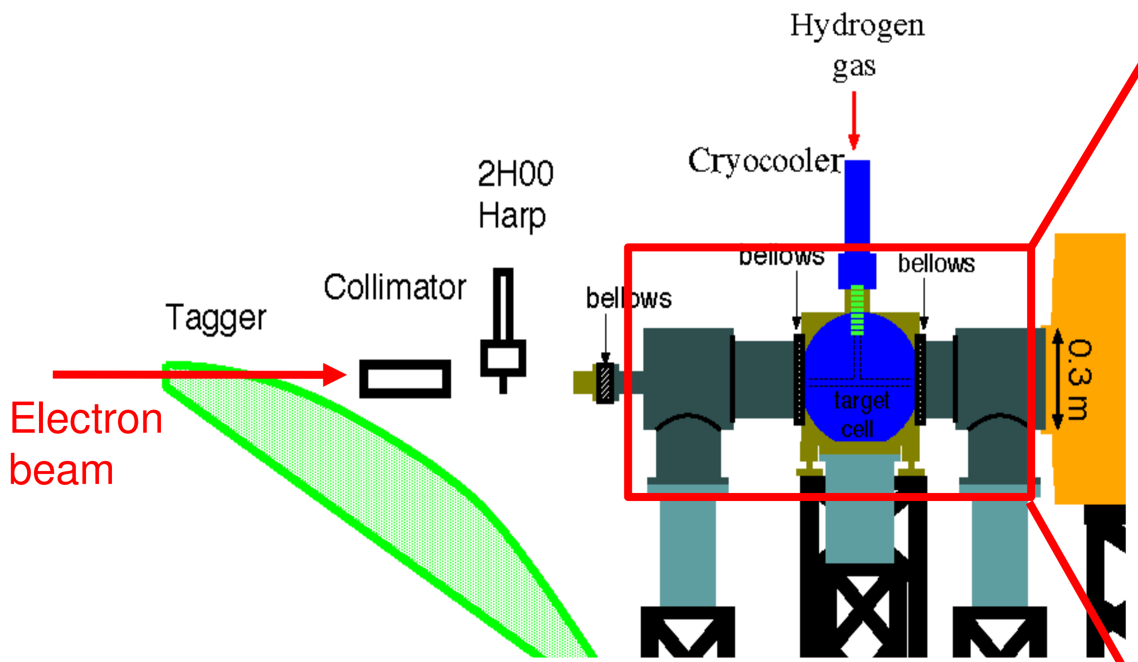

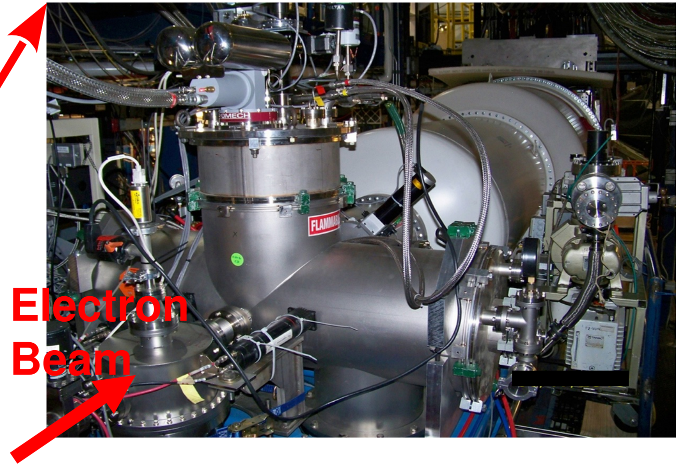

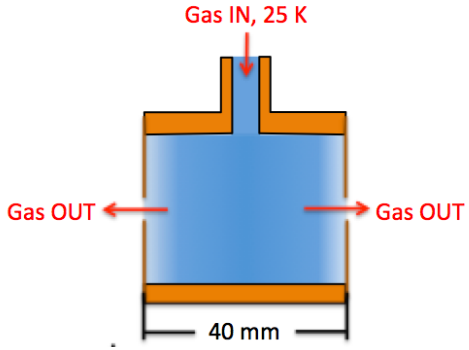

- 8 cm dia x 4 cm long target cell
- 2 mm holes open at front and back kapton foils, allows beam to pass through
- Target thickness: ~2 x 10^{18} H atoms / cm^2

PRad Experimental Apparatus

Hydrogen

E
b

PRad Setup (Side View)

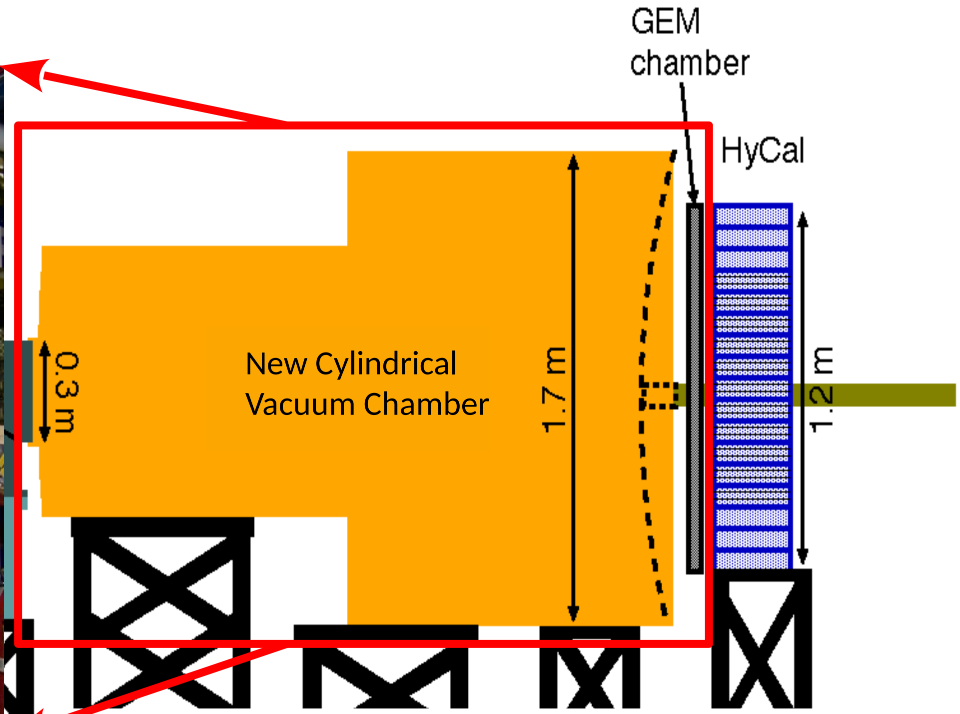

- 5 m long two stage vacuum chamber, further remove possible background source
- vacuum chamber pressure: 0.3 mTorr

PRad Experimental Apparatus

PRad Setup (Side View)

- Two large area GEM detectors
- Small overlap region in the middle
- Excellent position resolution (72 μm)
- Improve position resolution of the setup by > 20 times
- Large improvement for Q^2 determination

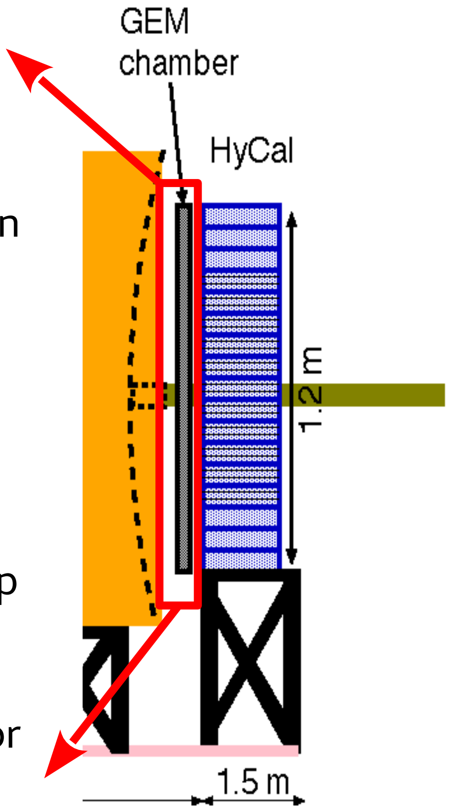

PRad Experimental Apparatus

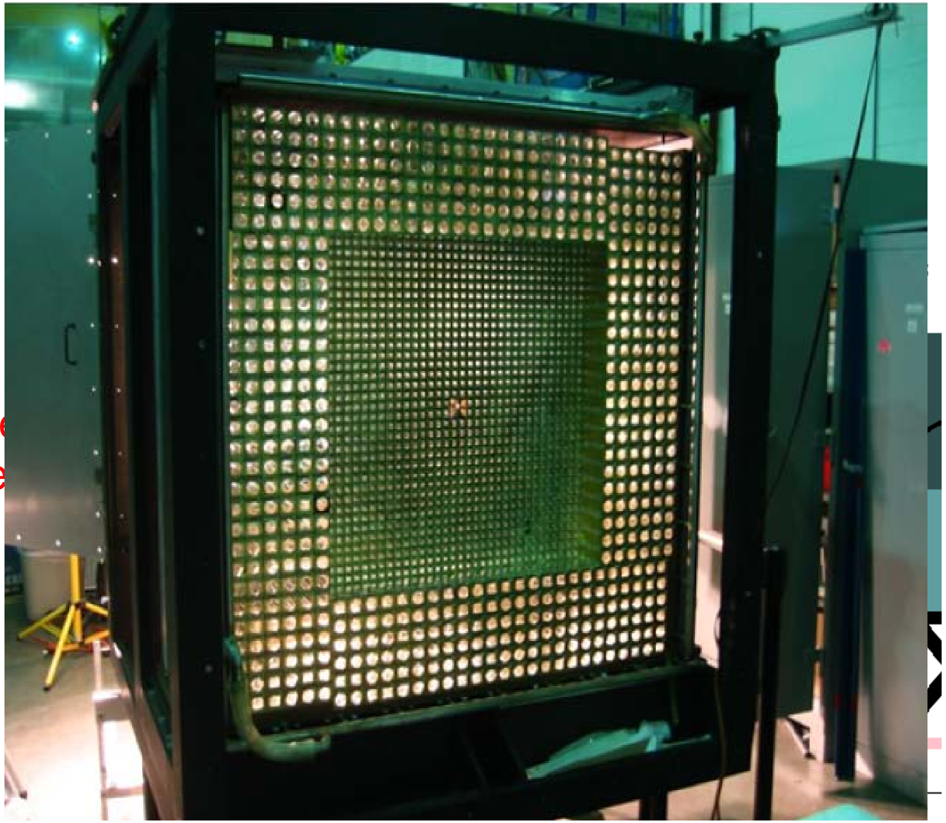

El
be

- Hybrid EM calorimeter (HyCal)
  - Inner 1156 PWO_4 modules
  - Outer 576 lead glass modules
- 5.8 m from the target
- Scattering angle coverage: ~ 0.6° to 7.5°
- Full azimuthal angle coverage
- High resolution and efficiency

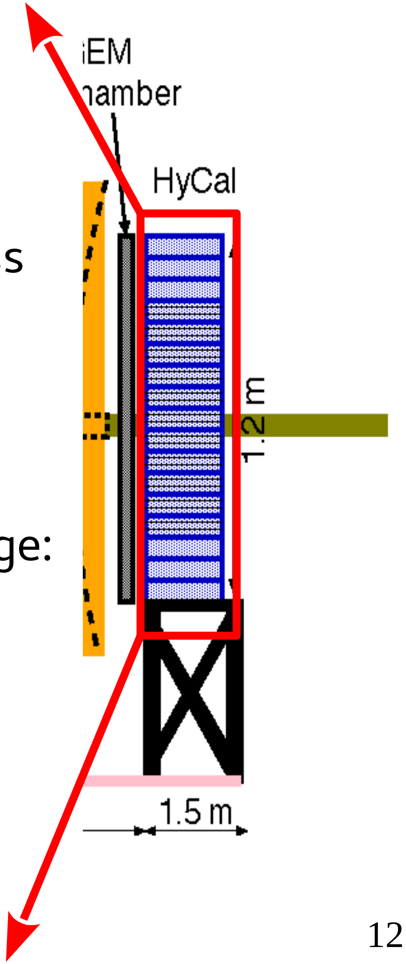

Extraction of ep Elastic Scattering Cross Section

- To reduce the systematic uncertainty, the ep cross section is normalized to the Møller cross section

$$\left(\frac{d\sigma}{d\Omega}\right)_{ep} = \left[\frac{N_{exp}(ep \rightarrow ep\ in\ \theta_i \pm \Delta\theta_i)}{N_{exp}(ee \rightarrow ee)} \cdot \frac{\epsilon^{ee}_{geom}}{\epsilon^{ep}_{geom}} \cdot \frac{\epsilon^{ee}_{det}}{\epsilon^{ep}_{det}}\right] \left(\frac{d\sigma}{d\Omega}\right)_{ee}$$

- Method1: bin by bin method – taking ep/ee counts from the same angle bin

  1) Cancellation of energy independent part of efficiency and acceptance
  2) Limited coverage due to double arm Møller acceptance

- Method2: integrated Møller method – integrate Møller in a fixed angle range, and use it as common normalization for all angle bins

- Luminosity canceled for both methods

Analysis - Event Selection

Event selection method

1. For all events, require hit matching between GEMs and HyCal
2. For *ep* and *ee* events, apply angle dependent energy cut based on kinematics
   1. Cut size depend on local detector resolution
3. For *ee*, if requiring double-arm events, apply additional cuts
   1. Elasticity
   2. Co-planarity
   3. Vertex z

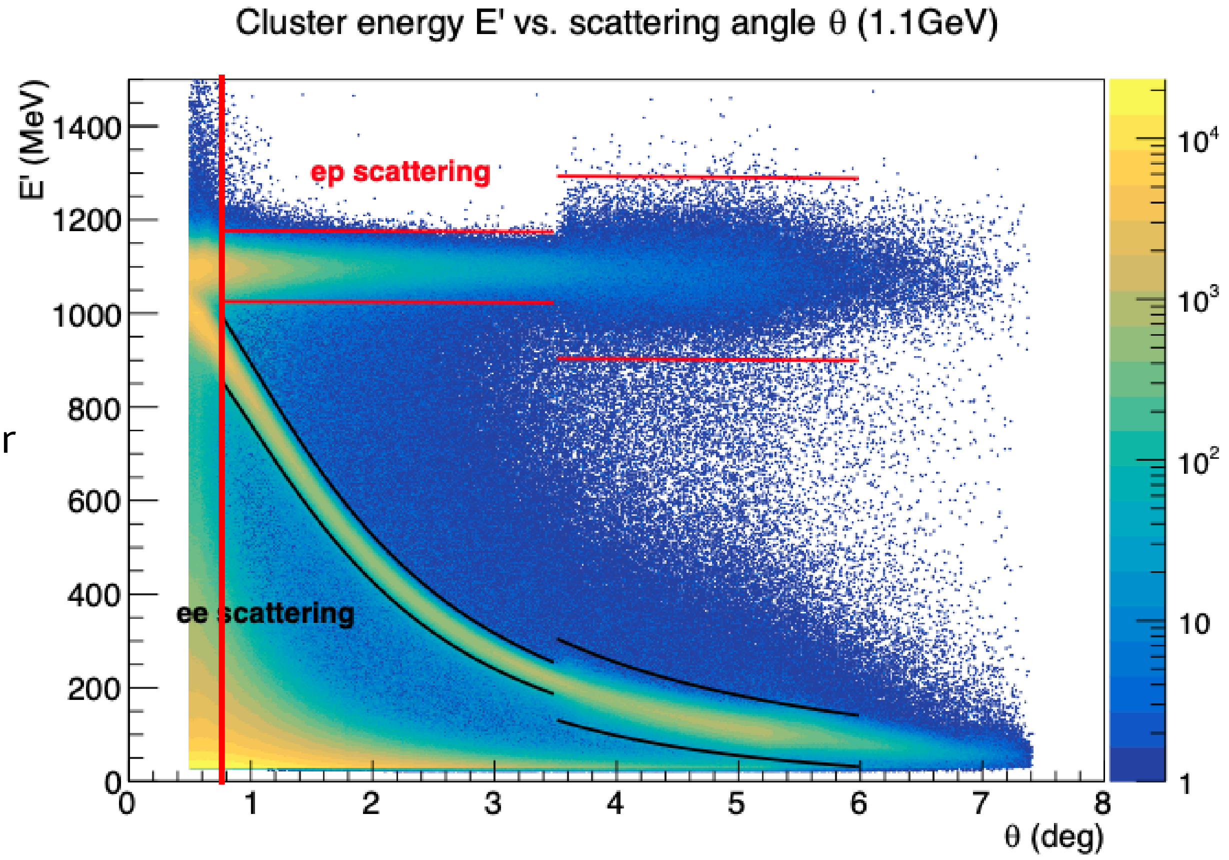

Extraction of ep Elastic Scattering Cross Section

- ep cross section is normalized to the Møller cross section

$$\left(\frac{d\sigma}{d\Omega}\right)_{ep} = \left[\frac{N_{exp}(ep \to ep\ in\ \theta_i \pm \Delta\theta_i)}{N_{exp}(ee \to ee)} \cdot \frac{\epsilon^{ee}_{geom}}{\epsilon^{ep}_{geom}} \cdot \frac{\epsilon^{ee}_{det}}{\epsilon^{ep}_{det}}\right] \left(\frac{d\sigma}{d\Omega}\right)_{ee}$$

- Method 1: bin by bin method – taking ep/ee counts from the same angle bin

  1) Cancellation of energy independent part of efficiency and acceptance
  2) Limited coverage due to double arm Møller acceptance

Cluster energy E' vs. scattering angle θ (1.1GeV)

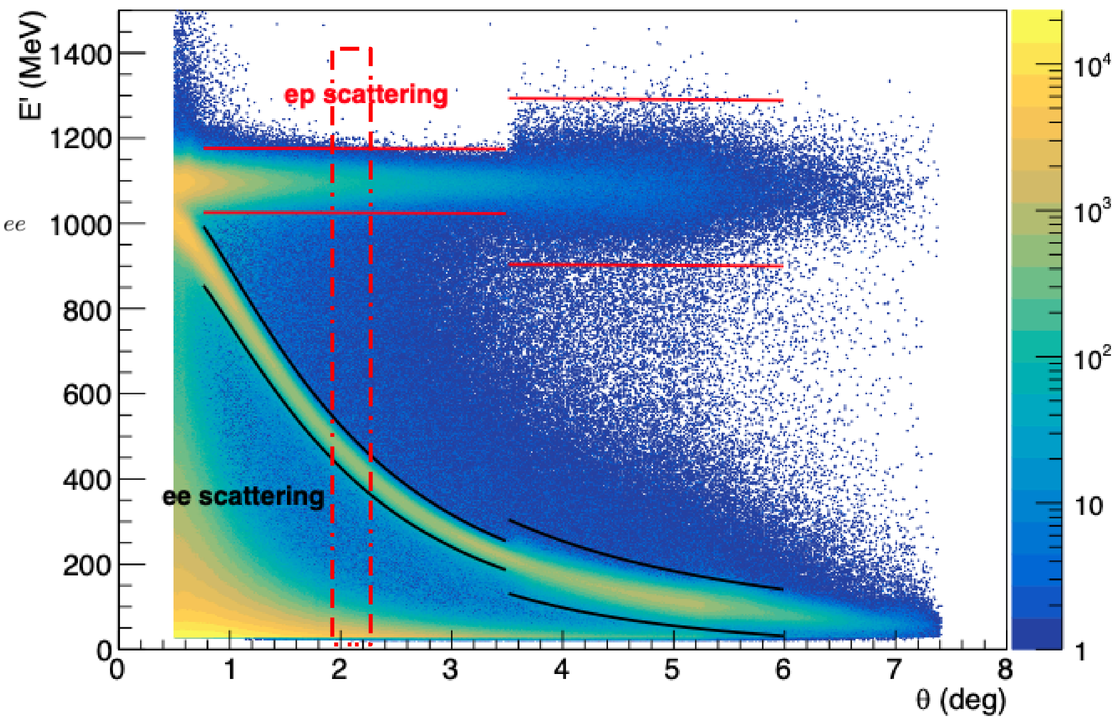

Extraction of ep Elastic Scattering Cross Section

- ep cross section is normalized to the Møller cross section

$$\left(\frac{d\sigma}{d\Omega}\right)_{ep} = \left[\frac{N_{exp}(ep \to ep\ in\ \theta_i \pm \Delta\theta_i)}{N_{exp}(ee \to ee)} \cdot \frac{\epsilon^{ee}_{geom}}{\epsilon^{ep}_{geom}} \cdot \frac{\epsilon^{ee}_{det}}{\epsilon^{ep}_{det}}\right] \left(\frac{d\sigma}{d\Omega}\right)_{ee}$$

- Method 2: integrated Møller method – integrate Møller in a fixed angle range, and use it as common normalization for all angle bins

- Luminosity canceled for both methods

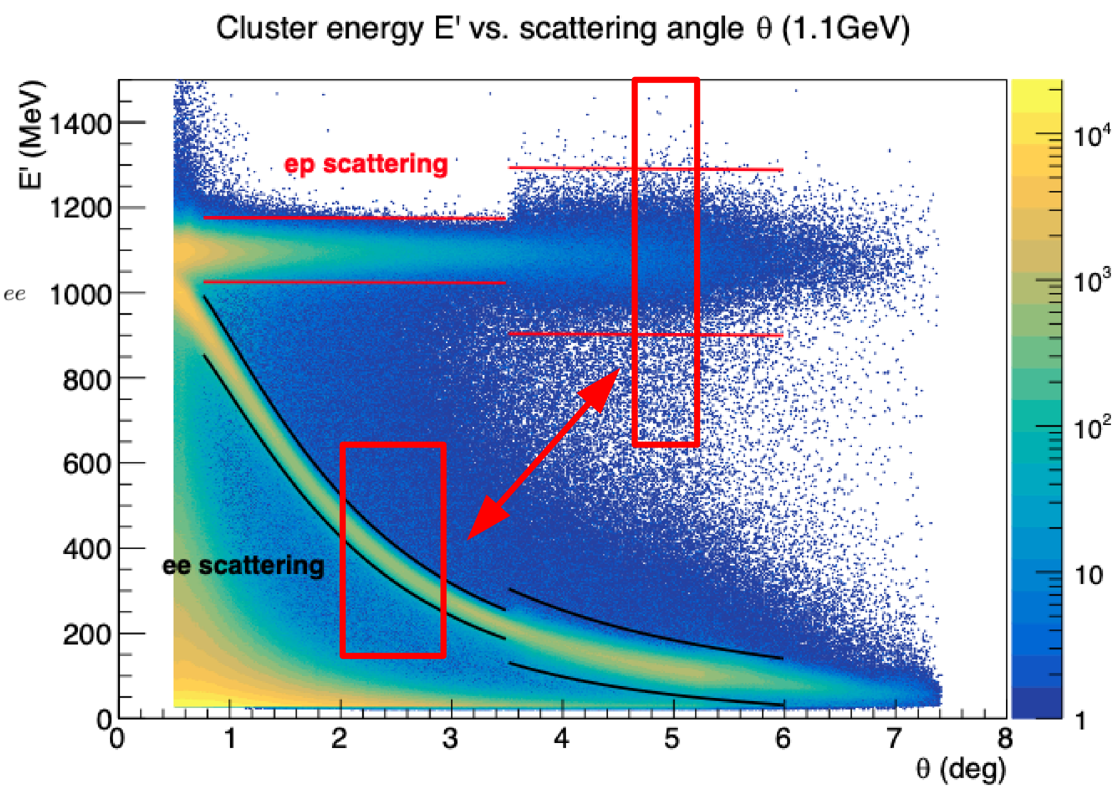

Analysis - Background Subtraction

- Data with different target configuration was taken for background subtraction and systematic uncertainty study
- Target density profile was fully simulated using COMSOL finite element analysis

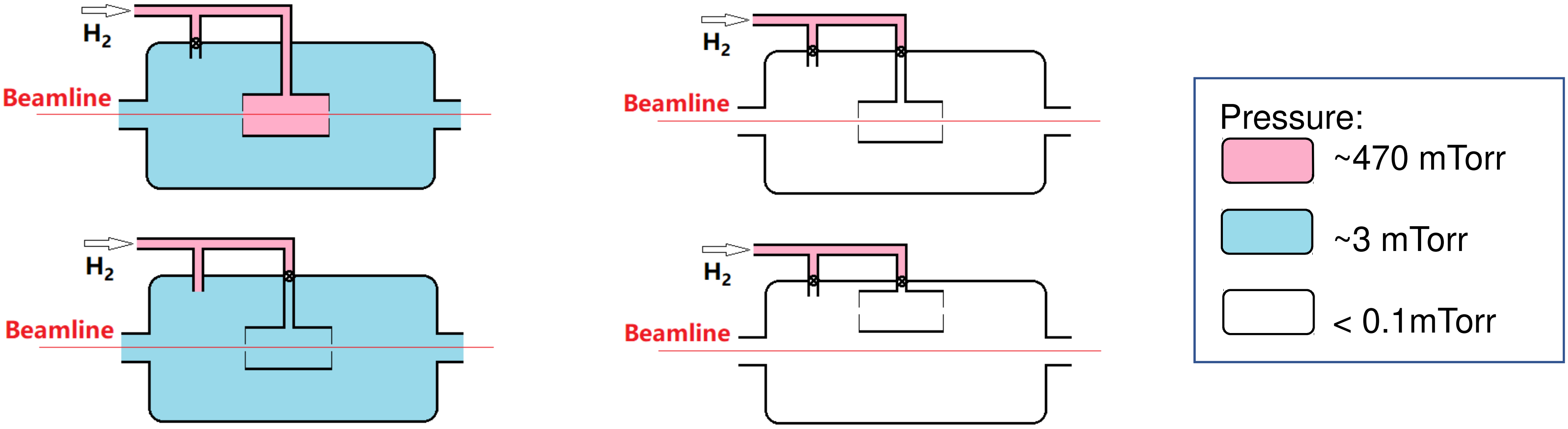

Analysis - Background Subtraction

- Data with different target configuration was taken for background subtraction and systematic uncertainty study
- Target density profile was fully simulated using COMSOL finite element analysis

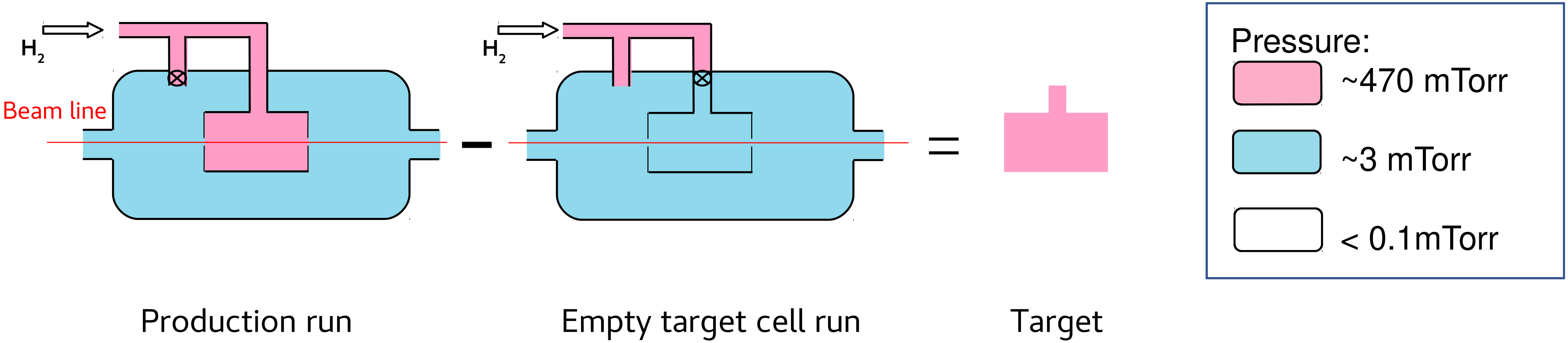

Background Subtraction

- ep background rate ~ 10% at forward angle (< 1.1 degree, dominated by upstream collimator), less than 2% at angles beyond 1.1 degree
- ee background rate ~0.8% at all angles

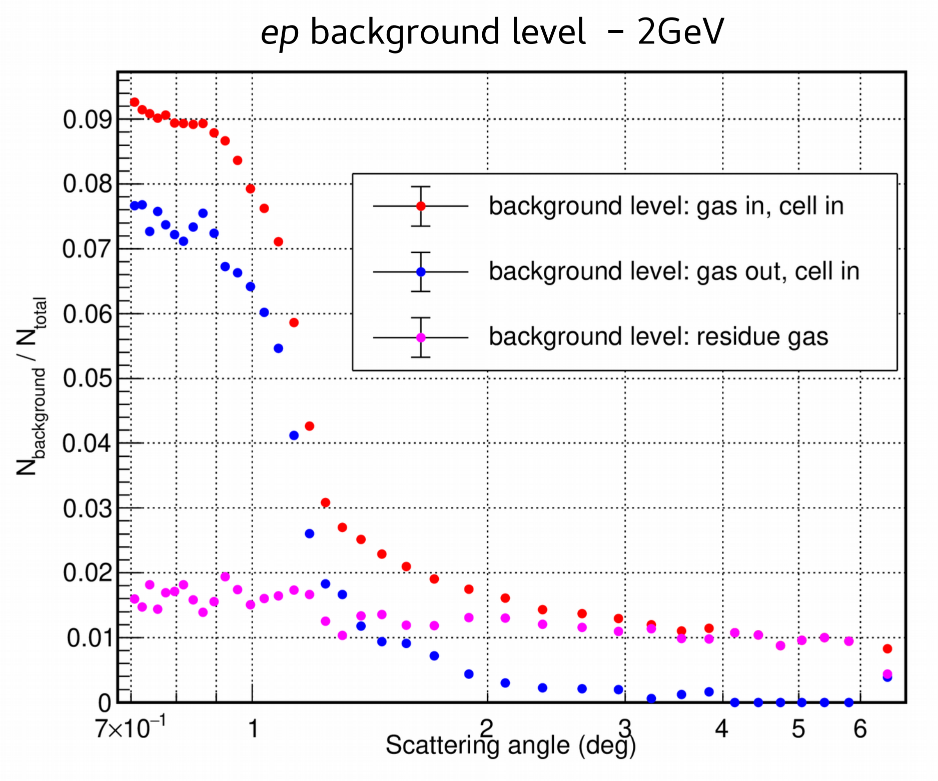

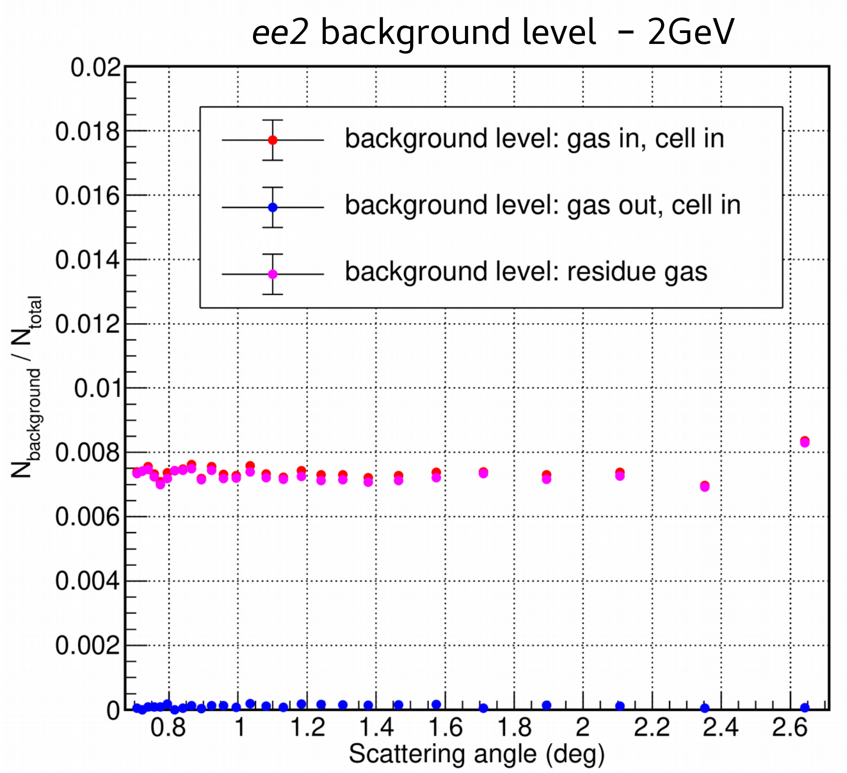

Background Subtraction

- ep background rate ~ 25% at forward angle (< 1.1 degree, dominated by upstream collimator), less than 5% at angles beyond 1.1 degree
- ee background rate ~2% at all angles

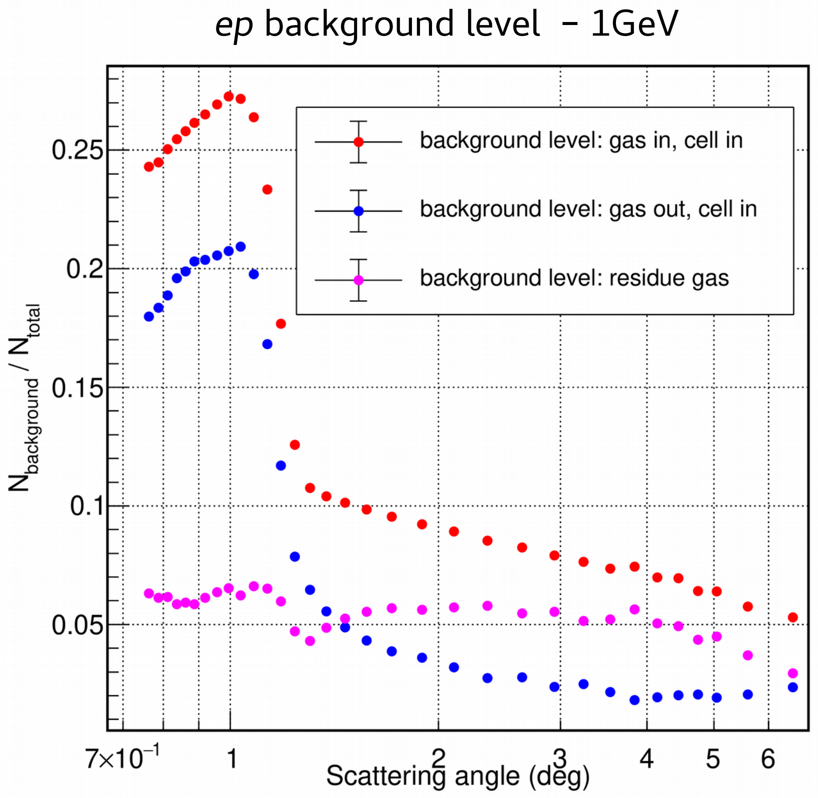

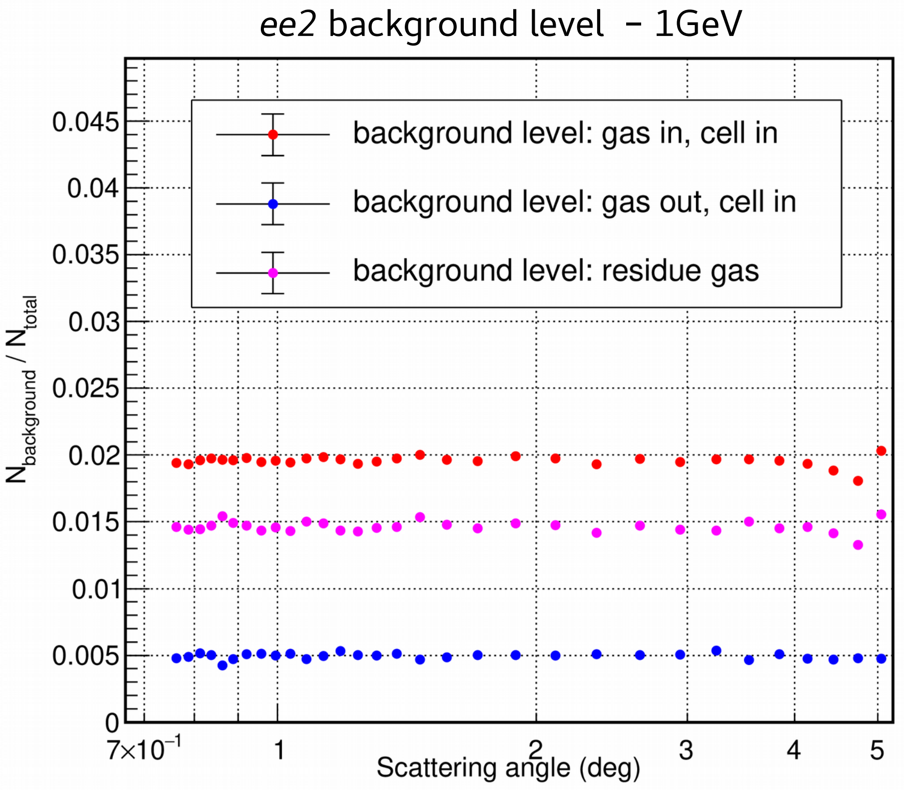

Inelastic Contribution

- Using Christy 2018 empirical fit to study inelastic ep contribution
- Good agreement between data and simulation
- Negligible for the PbWO4 region (<3.5), less than 0.2%(2.0%) for 1.1GeV(2.2GeV) in the Lead glass region

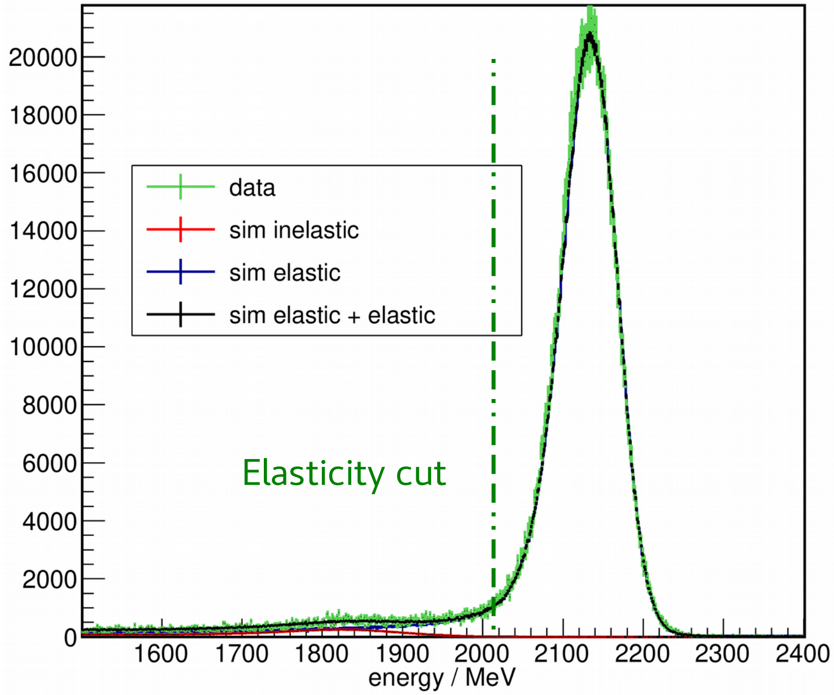

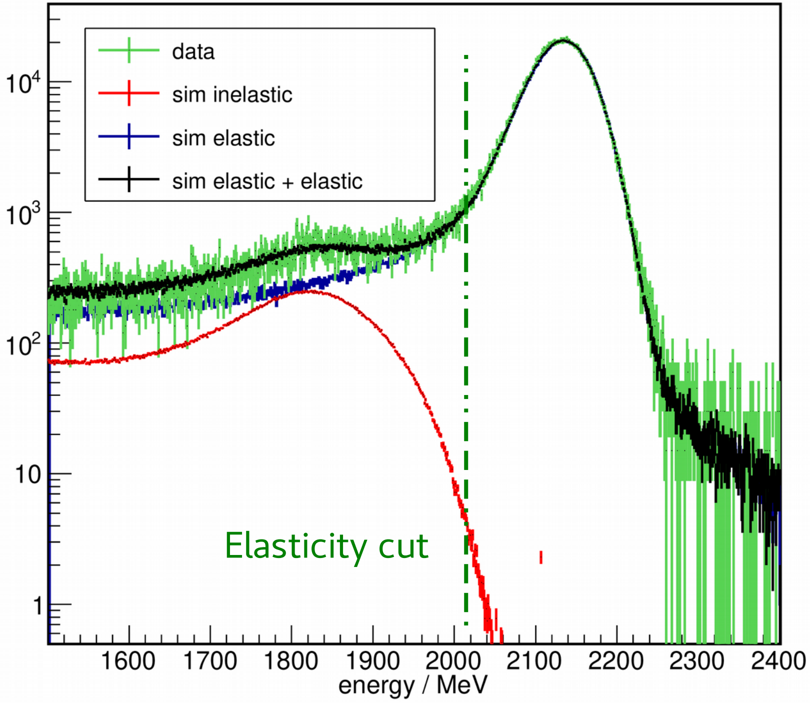

Radiative Correction

- Radiative effects corrected by Monte-Carlo method:

  1. Geant4 simulation package with full geometry setup
  2. Event generators with complete calculations of radiative corrections[1, 2], include emission of radiative photons
  3. Consistent results between generators
  4. Include TPE effect[3], less than 0.2% for ep in PRad kinematcis range
  5. Iterative procedure applied for radiative correction

$$\sigma_{ep}^{Born(exp)} = \left(\frac{\sigma_{ep}}{\sigma_{ee}}\right)^{exp} / \left(\frac{\sigma_{ep}}{\sigma_{ee}}\right)^{sim} \cdot \left(\frac{\sigma_{ep}}{\sigma_{ee}}\right)^{Born(model)} \cdot \sigma_{ee}^{Born(model)}$$

1. I. Akushevich et al., Eur. Phys. J. A 51(2015)1 (Fully beyond ultra relativistic approximation)
2. A. V. Gramolin et al., J. Phys. G Nucl. Part. Phys. 41(2014) 115001
3. O. Tomalak, Few Body Syst. 59, no. 5, 87 (2018)

Super Ratio

- Super ratio for 1.1 GeV and 2.2 GeV
- After iteration stablized

1.1 GeV data

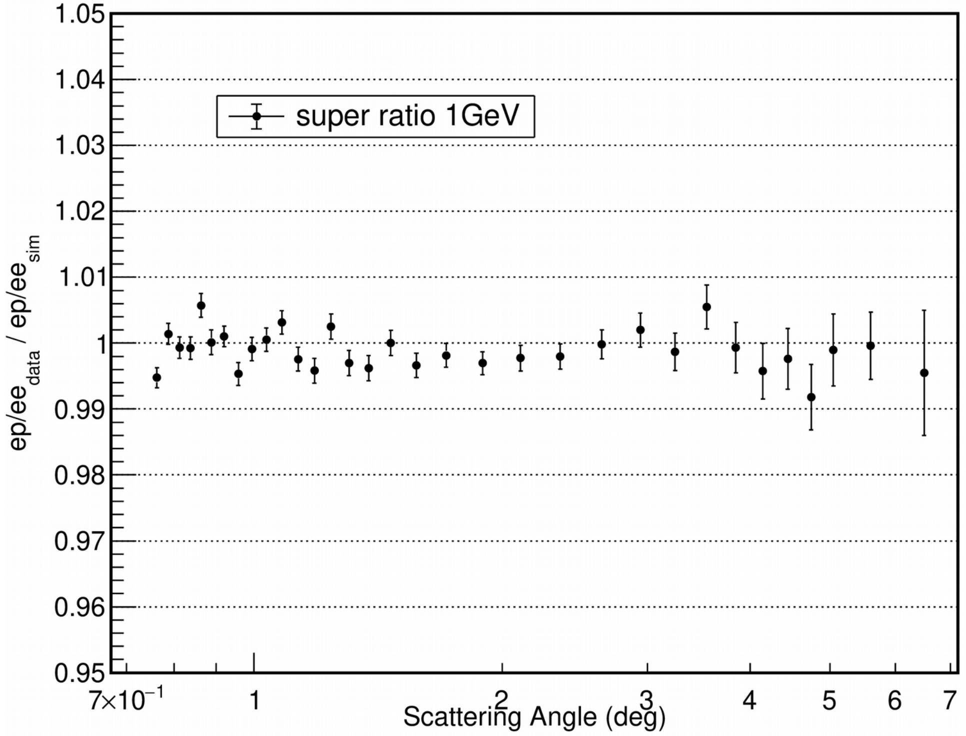

2.2 GeV data

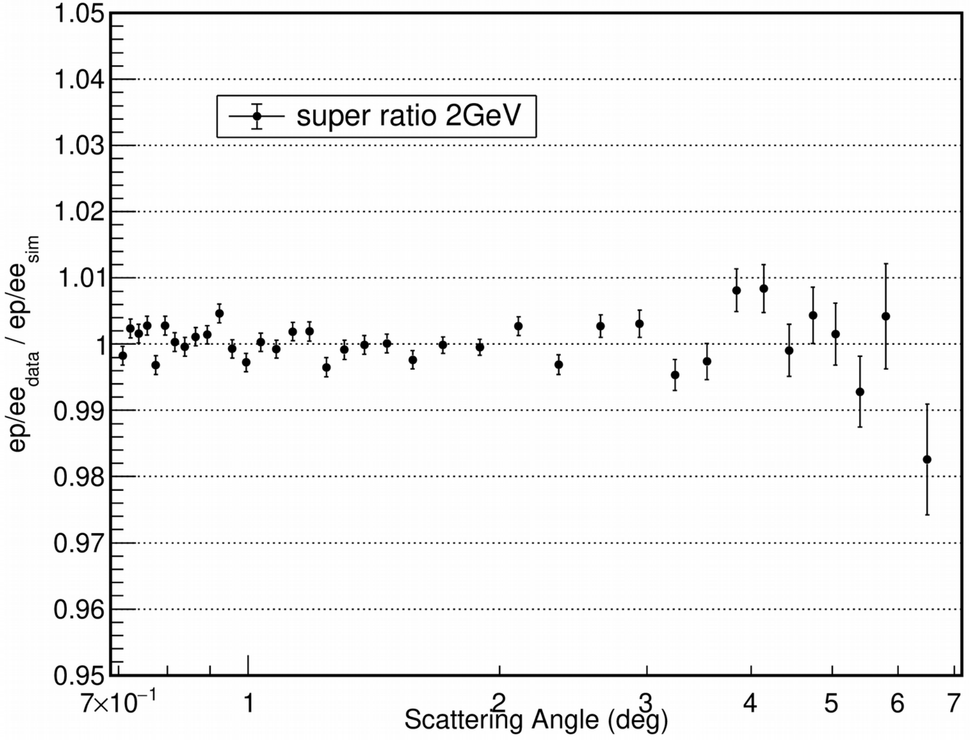

Differential Cross Section

- Extracted differential cross section v.s. Q^2, with 2.2 and 1.1 GeV data
- Statistical uncertainties: ~0.15% for 2GeV, ~0.2% for 1GeV per point
- Systematic uncertainties: 0.3% ~ 1.1% for 2GeV, 0.3 ~ 0.5% for 1GeV

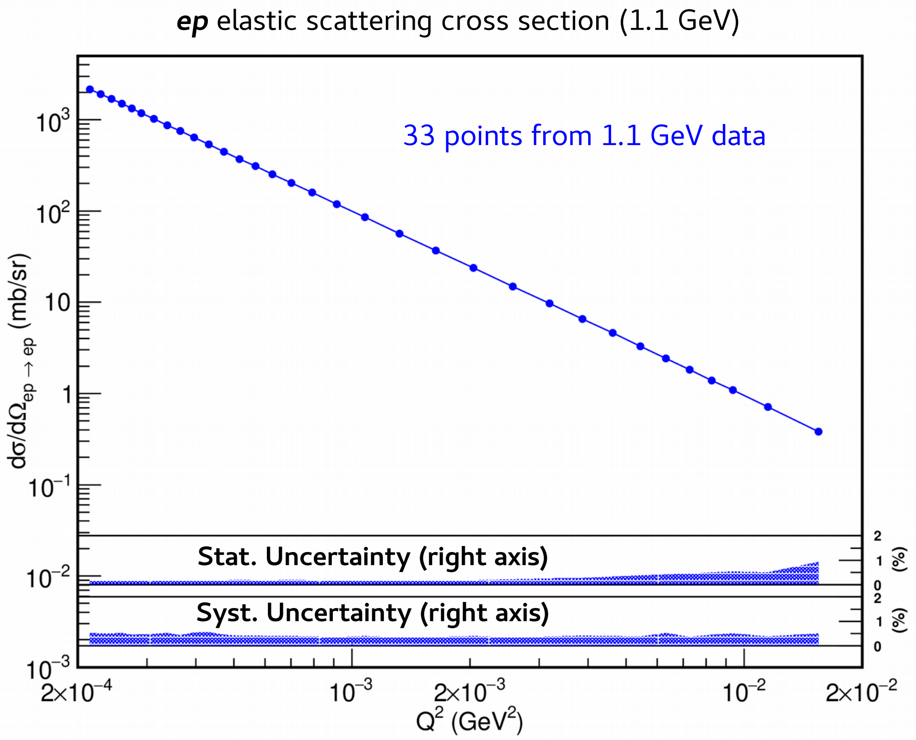

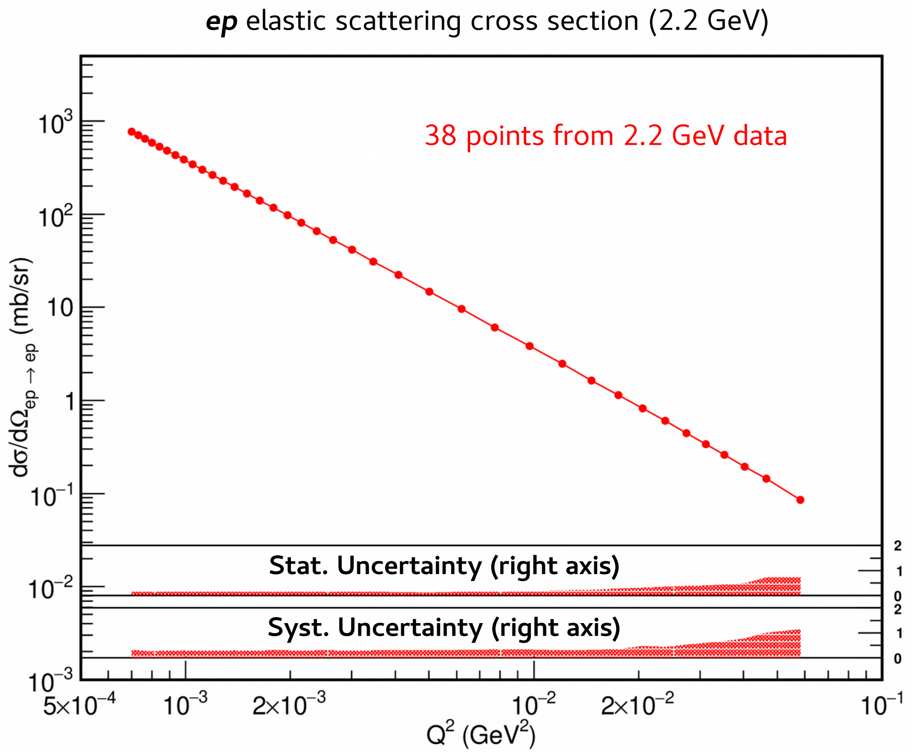

Electric Form Factor

- 33 points for 1GeV data
- 38 points for 2GeV data

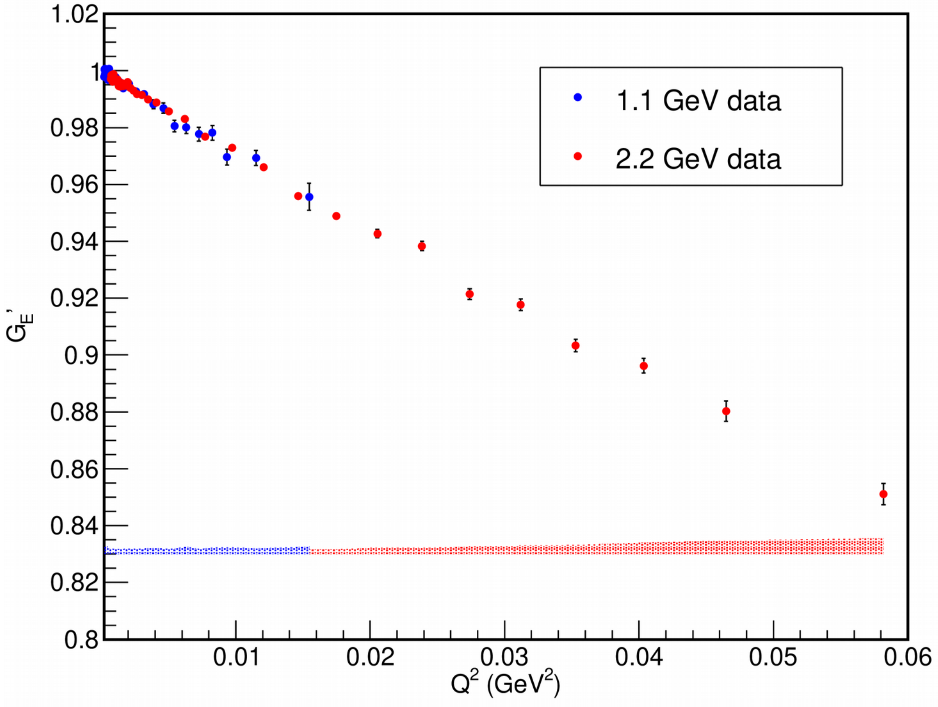

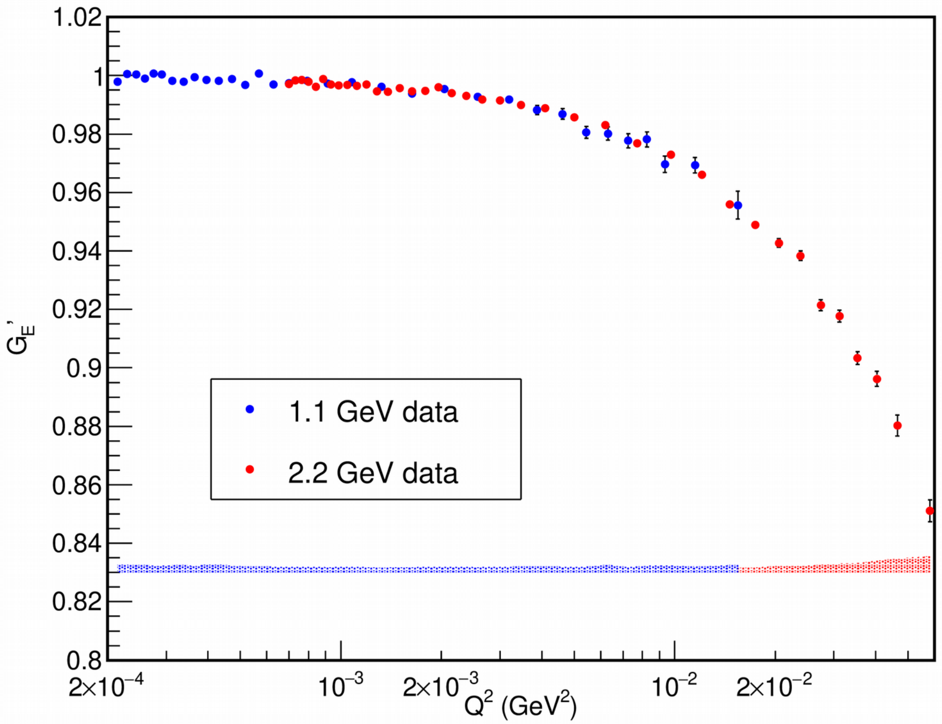

Form Factor Compare

- Two independent analysis tracks from Duke and UVa
- Radius results agree within statistical uncertainties

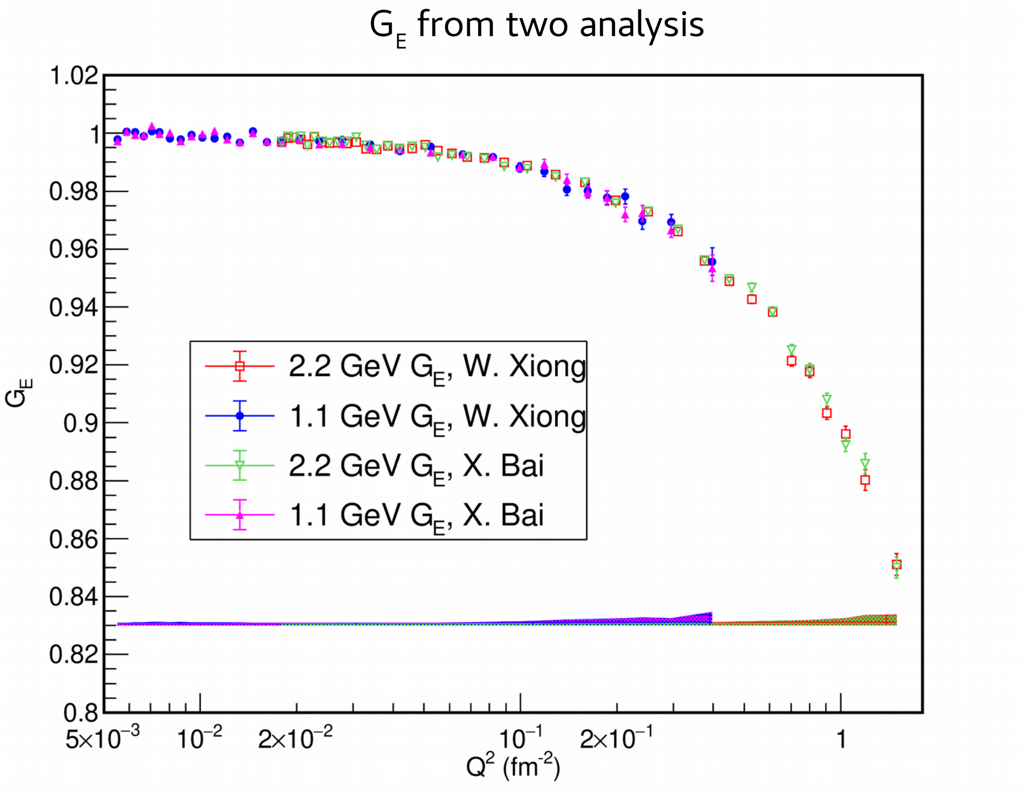

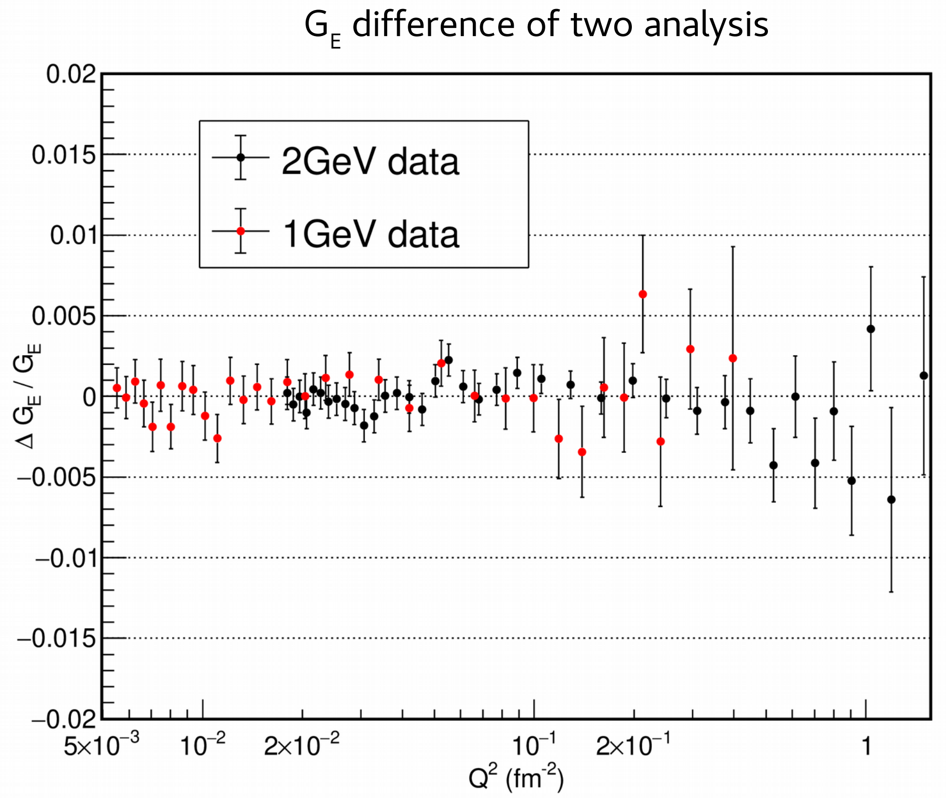

PRad G_E Expansion to the Word Data at Low Q^2

- 33 points for 1GeV data
- 38 points for 2GeV data

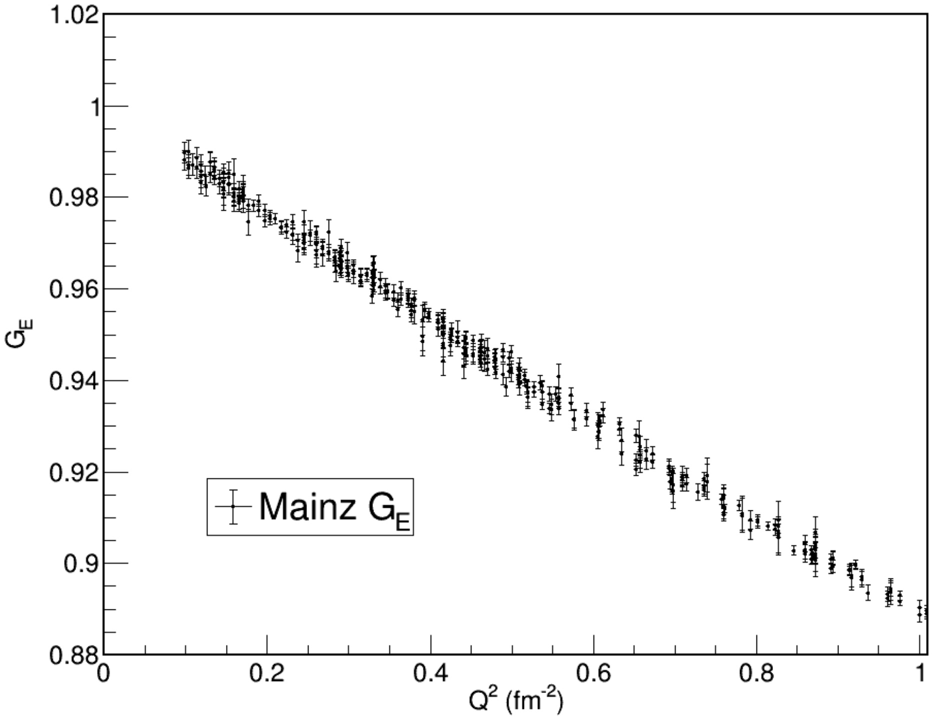

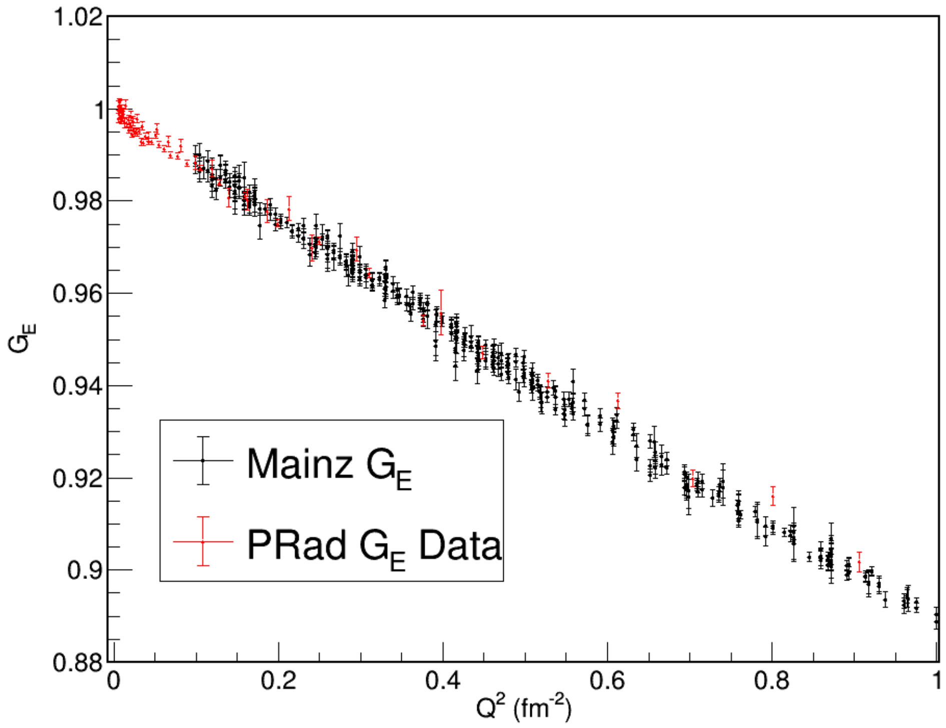

Searching the Robust Fitters

- Various fitters tested with a wide range of GE parameterizations, using Prad kinematic range and uncertainties
    - X. Yan et al. Phys. Rev. C98, 025204 (2018)

- Rational (1, 1), 2nd order z transformation and 2nd order continuous fraction are identified as robust fitters with reasonable uncertainties

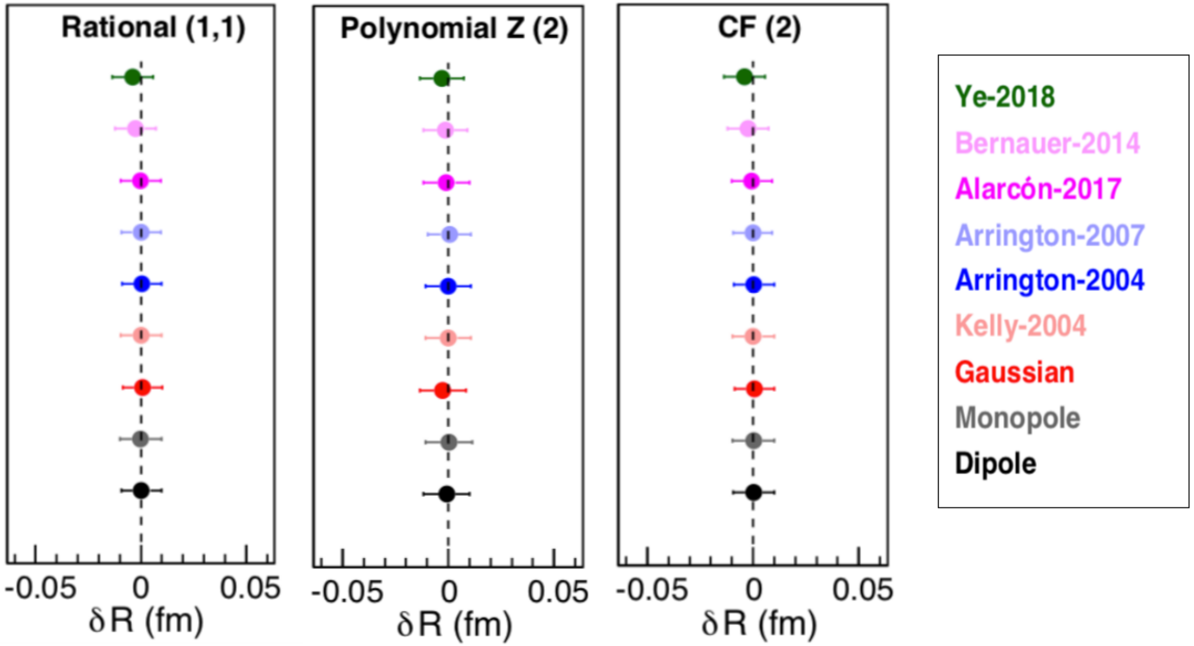

Rational (1,1)

$$p_0 \frac{1+p_1Q^2}{1+p_2Q^2}$$

2nd order *z* transformation

$$p_0(1+p_1 z+p_2 z^2)$$

$$z=\frac{\sqrt{T_c+Q^2}-\sqrt{T_c-T_0}}{\sqrt{T_c+Q^2}+\sqrt{T_c-T_0}}$$

2nd order continuous faction

$$p_0 \frac{1}{1+\frac{p_1Q^2}{1+p_2Q^2}}$$

The Radius Result

- n_1 and n_2 obtained by fitting PRad G_E to $\begin{cases} n_1 f(Q^2), & \text{for 1GeV data} \\ n_2 f(Q^2), & \text{for 2GeV data} \end{cases}$
- G'_E as normalized electric form factor: $\begin{cases} G_E/n_1, & \text{for 1GeV data} \\ G_E/n_2, & \text{for 2GeV data} \end{cases}$

X. Yan et al. PRC 98, 025204 (2018)

Using rational (1,1)

$$f(Q^2) = \frac{1 + p_1 Q^2}{1 + p_2 Q^2}$$

$$\left.\begin{array}{ll} R_p = 0.831 \pm 0.007\ (stat.) & \text{(Duke)} \\ R_p = 0.833 \pm 0.007\ (stat.) & \text{(UVa)} \end{array}\right\} \pm 0.012\ (syst.)\ fm$$

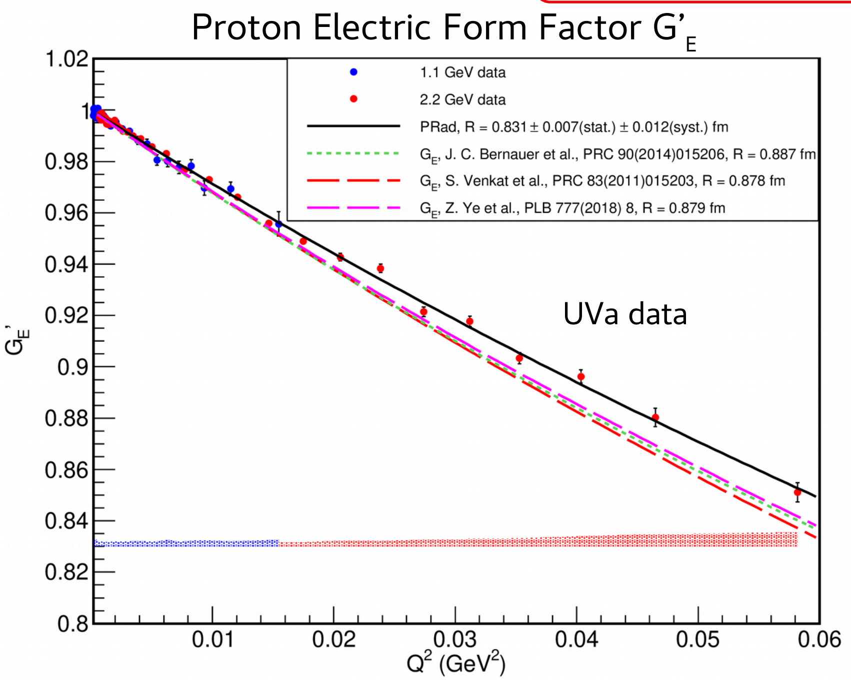

n_1 = 1.0002 +/- 0.0002(stat.) +/- 0.0020 (syst.),

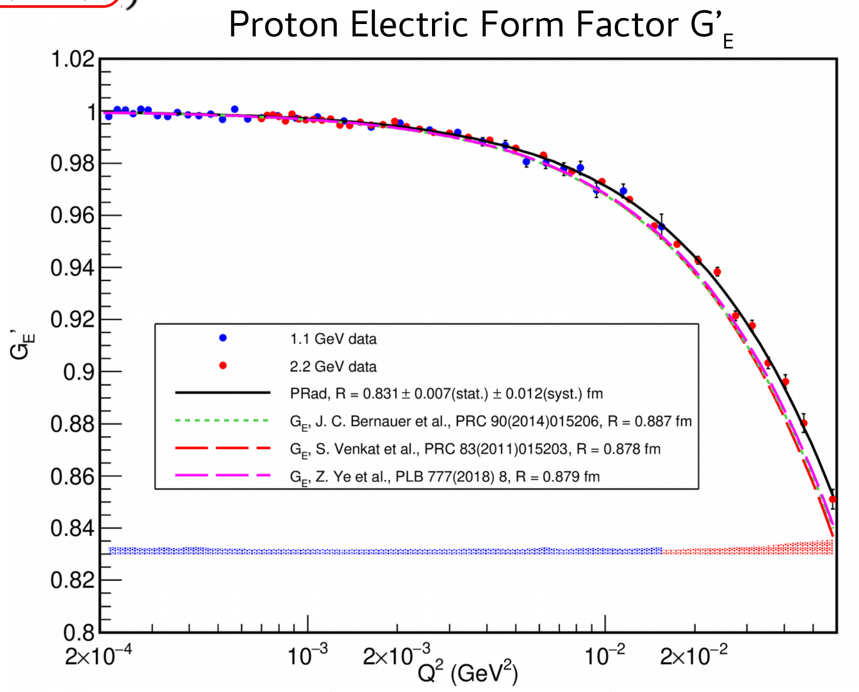

n_2 = 0.9983 +/- 0.0002(stat.) +/- 0.0013 (syst.)

Results Compare

- 2GeV cross section and form factor compare

Cross section compare – 2GeV

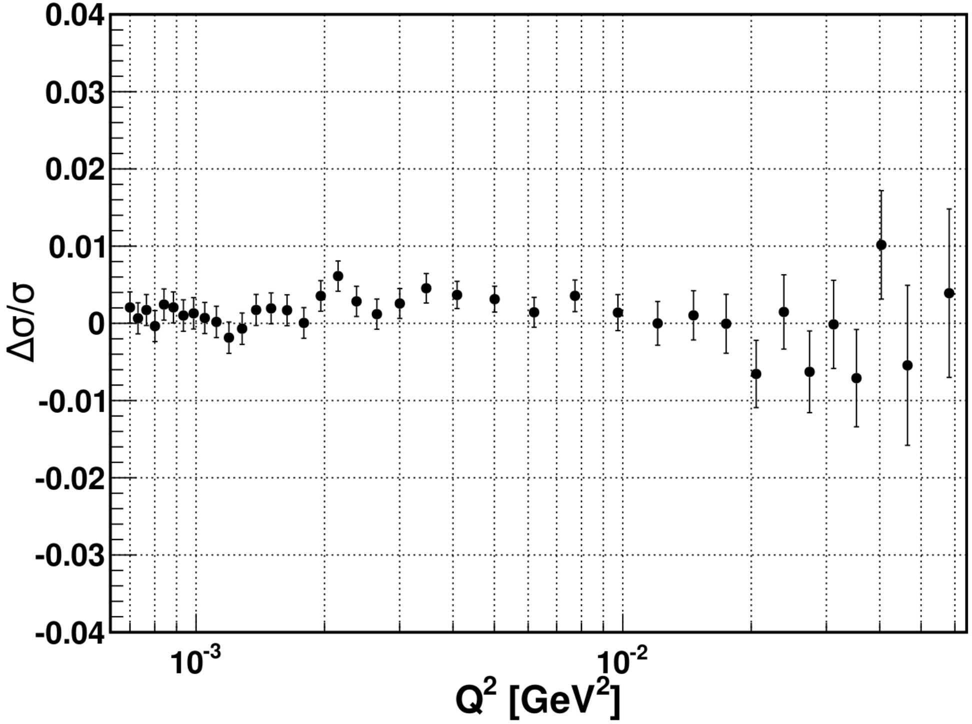

Form factor compare – 2GeV

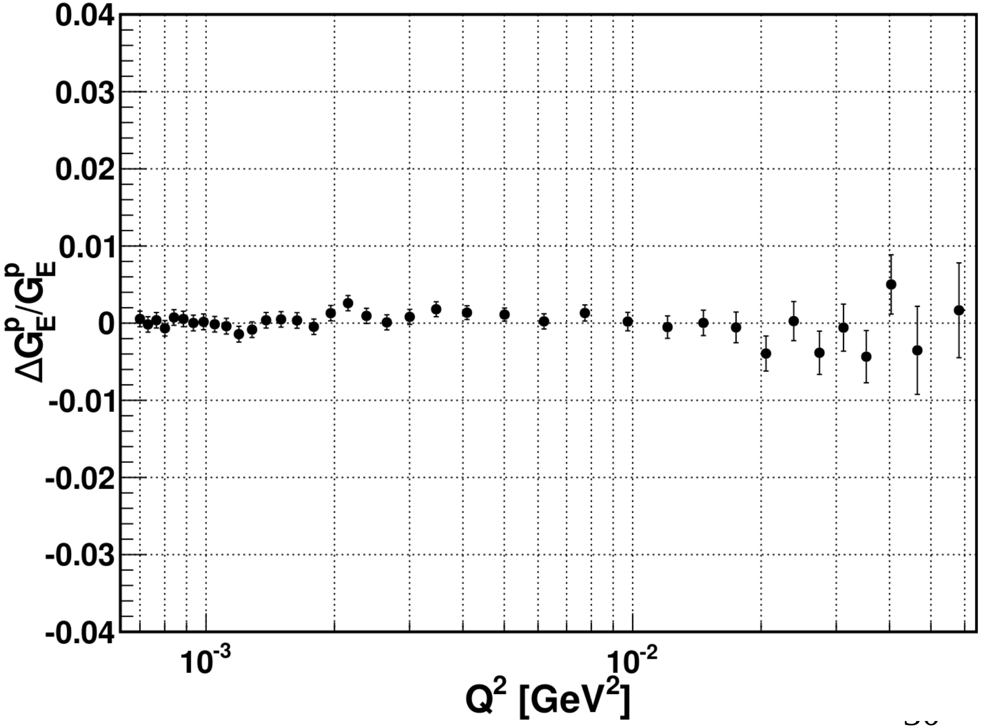

Results Compare

- 1GeV cross section and form factor compare

Cross section compare – 1GeV

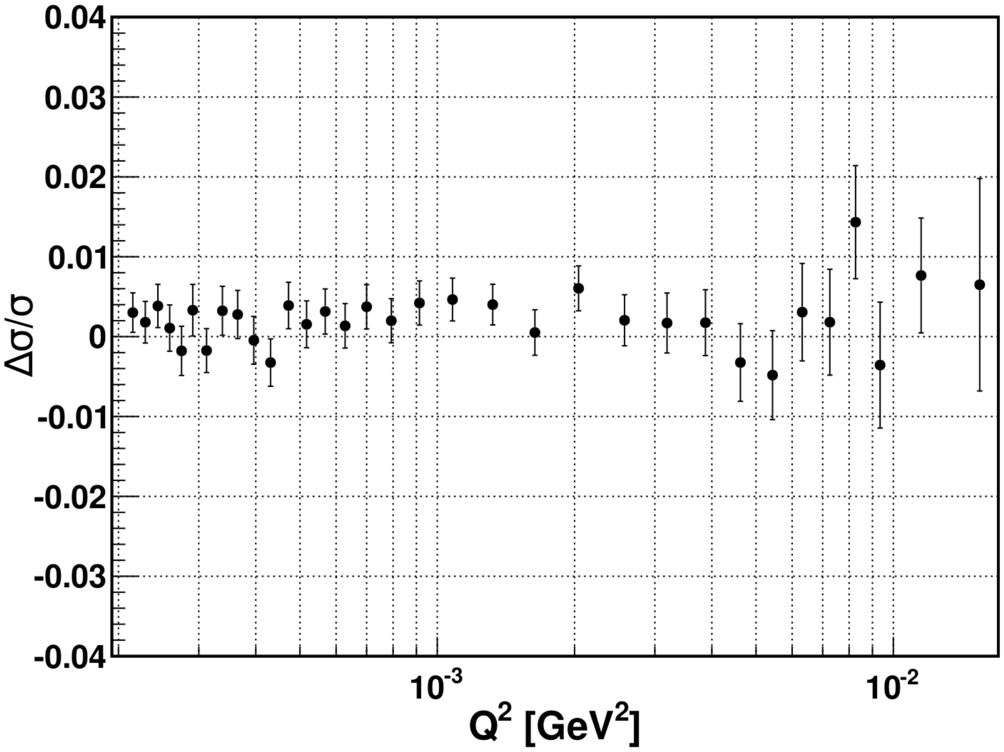

Form factor compare – 1GeV

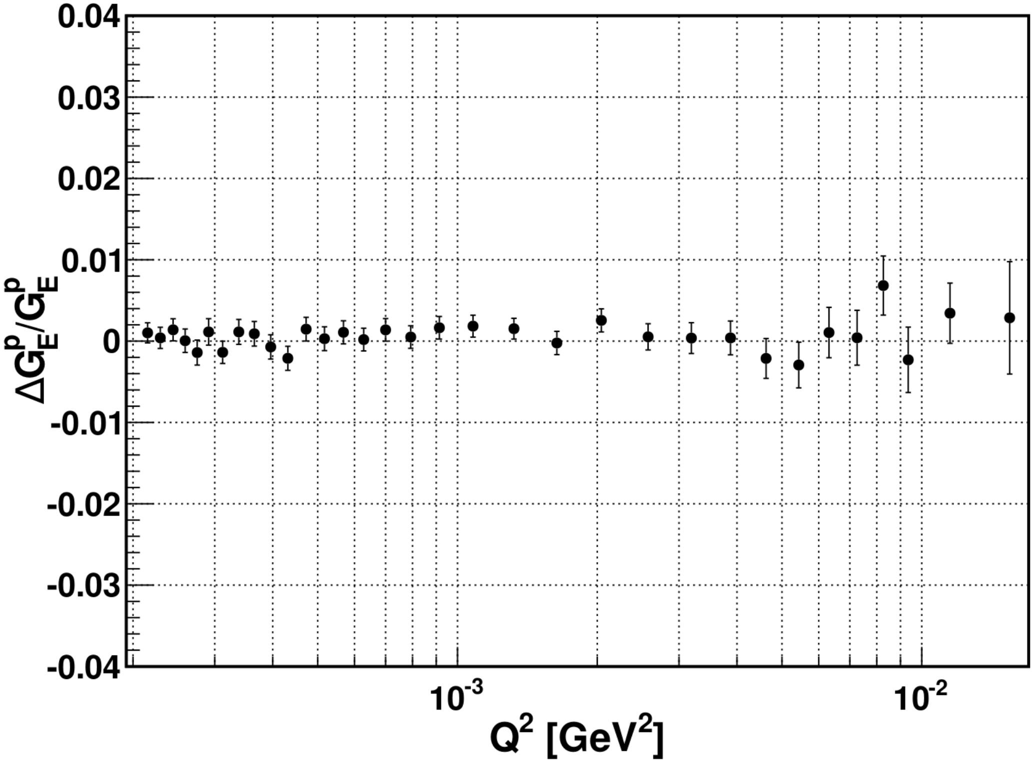

Systematic Uncertainties

- Major sources of systematic uncertainties

Item	R_p uncertainty (fm)	n_1 uncertainty	n_2 uncertainty
Event selection	0.0070	0.0002	0.0006
Radiative correction	0.0069	0.0010	0.0011
Detector efficiency	0.0042	0.0000	0.0001
Beam background	0.0039	0.0017	0.0003
HyCal response	0.0029	0.0000	0.0000
Acceptance	0.0026	0.0001	0.0001
Beam energy	0.0022	0.0001	0.0002
Inelastic ep	0.0009	0.0000	0.0000
Total	0.0116	0.0020	0.0013

Table courtesy: W. Xiong

PRad Results on the Radius

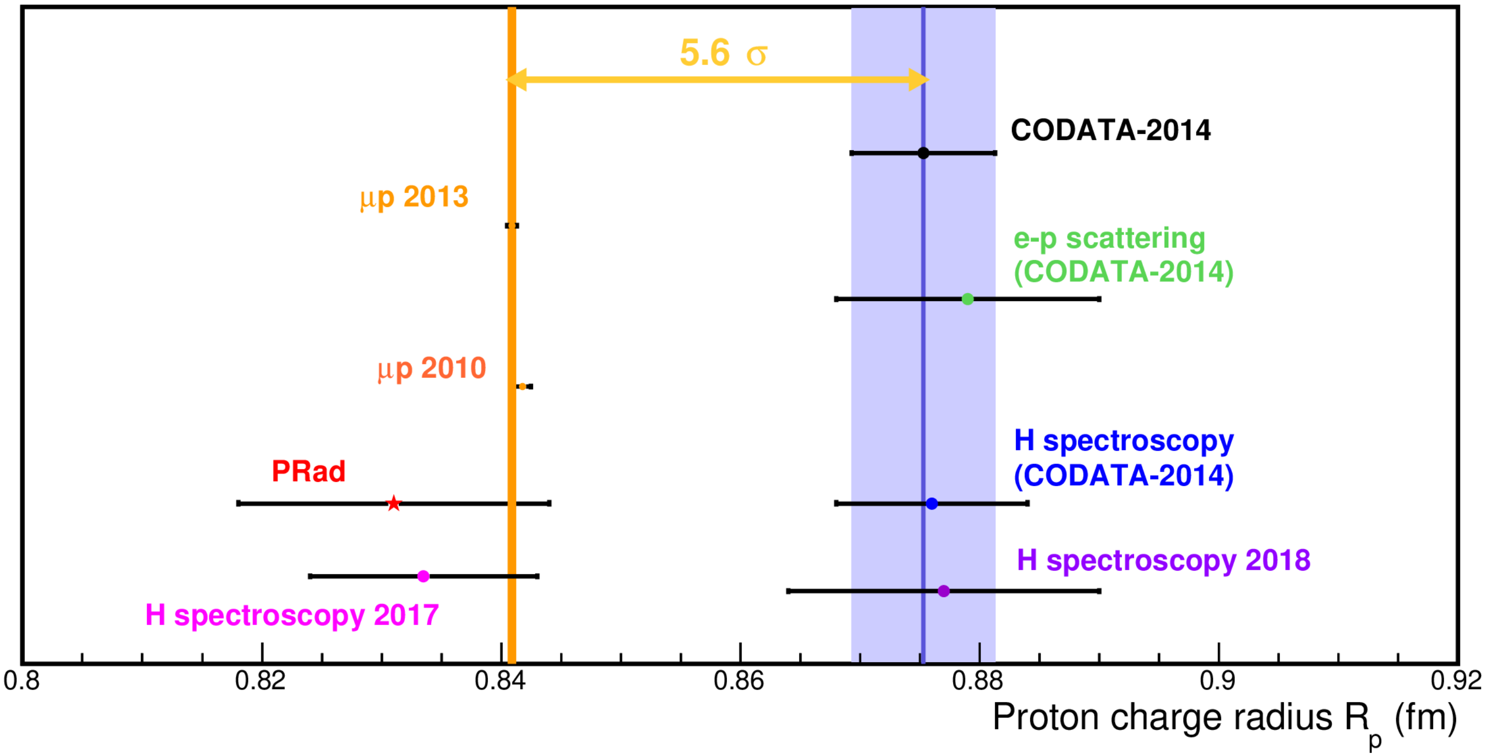

Summary

- The PRad result:

$$\left.\begin{array}{ll} \color{red}{R_p = 0.831 \pm 0.007\ (stat.)} & \text{(Duke)} \\ \color{blue}{R_p = 0.833 \pm 0.007\ (stat.)} & \text{(UVa)} \end{array}\right\} \color{red}{\pm 0.012\ (syst.)\ fm}$$

- After almost 10 years, the proton radius puzzle remains interesting

- The PRad Collaboration carried out a first electron scattering experiment using a non-magnetic spectrometer approach – calorimeter and GEMs

  1. Covers two orders of magnitude in low Q^2 with the same detector setting
  2. Unprecedented low Q^2 data set (~ 2×10^{-4} GeV^2) has been collected in ep elastic scattering experiment
  3. Simultaneous measurement of ep and ee scattering to reduce systematics
  4. Novel use of a window-less cryogenically cooled hydrogen gas target